

Growth of $(\text{Na}_{0.5}\text{K}_{0.5})\text{NbO}_3$ single crystals by abnormal grain growth method from special shaped nano-powders

Chao Wang, Yu-Dong Hou*, Hai-Yan Ge, Man-Kang Zhu, Hui Yan

Key Laboratory of Advanced Functional Materials of China Education Ministry, College of Materials Science and Engineering, Beijing University of Technology, Beijing 100124, People's Republic of China

Received 2 September 2009; received in revised form 14 December 2009; accepted 6 January 2010

Available online 29 January 2010

Abstract

Using the composite powders of $(\text{Na}_{0.5}\text{K}_{0.5})\text{NbO}_3$ (NKN) nano-particles and nano-rods as starting materials, the NKN single crystals were prepared by abnormal grain growth (AGG) method. The morphology evolution and the formation mechanism in the crystal growth process were investigated in detail. The results revealed that the average size and the apparent quantity of abnormal grains increased gradually with the increase of sintering temperature. The biggest NKN single crystals with size of about 3 mm were obtained at 950 °C for 2 h. Though the nano-particles and nano-rods have the same composition, the driving forces are distinctively different due to the diversity of grain morphology. The nano-rods have the large driving forces especially at high sintering temperature, which plays a dominant role in facilitating the formation of NKN single crystals during AGG process.

© 2010 Elsevier Ltd. All rights reserved.

Keywords: Niobates; Sol–gel processes; Microstructure-prefiring; Sintering; Abnormal grain growth

1. Introduction

Lead-based piezoelectric materials such as $(\text{Pb}, \text{Zr})\text{TiO}_3$ (PZT) are most used in acoustic transducers, medical ultrasonic probes, solid actuators, and other electromechanical fields due to their excellent piezoelectric properties.^{1,2} However, the toxicity of lead oxide has led to a demand for alternative lead-free piezoelectric materials. The main research works are now focused on alkali niobates, modified bismuth titanates, and systems which have a Morphotropic Phase Boundary (MPB) structure.^{3–6} Among these systems, alkaline niobate $(\text{Na}_{0.5}\text{K}_{0.5})\text{NbO}_3$ (NKN) based solid solutions, which have large piezoelectric response and strong ferroelectricity, are considered to be a potential substitute for lead-based piezoelectric materials. However, due to the volatility of potassium element and lack of pyroplastic behavior, it is hard to obtain dense alkaline niobate ceramics by the conventional method.⁷

In 2004, a great breakthrough has been made in alkaline niobate systems.^{8–10} Saito et al. have synthesized the compacted

textured NKN-based ceramics using reactive templated grain growth (RTGG) method. The properties of the obtained NKN textured ceramics are much better than that of the non-textured form, and can be compared to that of PZT4. So, it is natural to anticipate that NKN-based single crystals might have even better piezoelectricity than their textured forms for the optimal crystallographic orientation and domain structure in the single crystal body.¹¹ However, until now, there are few works concentrated on the crystal growth of NKN, which might be due to the high cost and tedious process in the normal crystal growth methods.^{11–13}

Solid-state single crystal growth method has been widely used in the fabrication of single crystals of various metallic materials, barium titanate, PMN-PT and NKN.^{14–20} Abnormal grain growth (AGG) is one of the solid-state single crystal growth methods, which is highly promising particularly for materials with a high melting temperature, phase transition, volatile elements and incongruent melting.²¹ It is anticipated that NKN-based single crystals would be obtained by AGG method through adjusting the process carefully. Recently, several papers have reported the AGG phenomena in NKN-based ceramics.^{22–24} However, the precursor oxide powders used in all these studies are prepared by conventional solid-state method. Due to the

* Corresponding author. Tel.: +86 10 67392445; fax: +86 10 67392445.
E-mail address: ydhoul@bjut.edu.cn (Y.-D. Hou).

high calcining temperature, the synthesized powders have the large size (normally in micrometer scale) with strong agglomeration, which pertain the low sintering ability and prohibit the effective growth of NKN crystal. Normally, the size of abnormal grown grain was below a millimeter. As we know, nano-sized powders have a higher inherent surface area, which provides a significantly higher driving force for grain growth. That is to say, using nano-powders as starting materials, it can be anticipated to obtain the large size of NKN-based single crystals by AGG method under lower sintering temperature. To our best of knowledge, the crystal growth of NKN-based nano-powders in AGG process have not been reported previously.

In this study, special shaped (mixture of particles and rods) NKN nano-powders were synthesized by the developed sol–gel method. By using these powders as starting materials, a millimeter sized NKN single crystals were successfully prepared. The grain growth mechanism in AGG process has also been investigated in detail.

2. Experimental procedure

Na_2CO_3 (99.8%), K_2CO_3 (99%), citric acid ($\text{C}_6\text{H}_8\text{O}_7 \cdot \text{H}_2\text{O}$, 99.5%) and acetic acid (CH_3COOH , 99.5%) were used as raw materials in combination with a water-soluble niobate solution.²⁵ The nano-sized NKN powders were prepared by sol–gel method, and the scheme was as follows. According to the chemical stoichiometry of NKN, the water-soluble niobate solution was mixed with Na_2CO_3 and K_2CO_3 , into a diluted solution of citric acid, and subsequently acetic acid was added to control the pH value. Before gaining the homogeneous yellow sol, vigorous stirring for 2 h was required. Thereafter, the sol was heated at 80 °C for 12 h to prepare dried gels. Then the dried gels were calcined at 500 °C for 5 h with a heating rate of 5 °C/min to obtain NKN nano-sized powders.

Using these nano-sized powders, the NKN ceramics were prepared by conventional sintering as follows. The powders were granulated with poly(vinylalcohol) and pressed into disks of 11.5 mm diameter followed by a uniaxial pressing under 450 MPa. These powder compacts were sintered in air at different sintering temperatures between 750 °C and 950 °C. For crystal phase and morphology analyses, the surfaces of ceramics were mirror polished carefully.

The crystal phases of the powders and ceramics were determined using X-ray diffractometry (XRD; Model D8 Advance, Bruker AXS, Karlsruhe, Germany) in θ – 2θ mode with graphite monochromatized Cu $\text{K}\alpha$ radiation ($\lambda = 0.154178$ nm). The optical and polarizing micrographs were obtained by an Olympus BX51 M microscope (Olympus, Tokyo, Japan). Abnormal grain size distribution was measured from the photographs of the ceramic surfaces by image processing software (Photoshop CS 8.0.1, Adobe, CA, USA). The equivalent spherical two-dimensional grain radii were measured and converted to equivalent spherical three-dimensional grain radii by dividing by 0.76.²⁶ Transmission electron microscopy (TEM) and selected-area electron diffraction (SAED) were carried out using a JEM-2000 F TEM (JEOL, Tokyo, Japan). Samples for TEM were firstly grounded mechanically to about 50 μm thickness,

and then thinned to perforation by the argon-ion milling method. Micromorphology of samples was studied using scanning electron microscope (SEM; Model S-3500N, Hitachi, Tokyo, Japan). For SEM experiments, the ceramic samples were mechanically fractured and coated with aurum film to facilitate the observation.

3. Results and discussion

Fig. 1(a) shows the XRD pattern of the NKN powders synthesized by sol–gel method. It can be seen that only a pure NKN orthorhombic phase could be discovered and there was no evidence of a second phase. Fig. 1(b) shows the TEM image of these NKN powders. The morphology of the powders shows a composite structure of particles and rods, which is different from the observation of homogeneous NKN nano-particles in the former work.²⁵ It was found that the morphology of the NKN powders is strongly determined by the calcining procedure. By adjusting appropriate heating rate, inhomogeneous shapes of NKN powders were synthesized and the detailed crystallization process of the powders will be investigated in other articles. As shown in Fig. 1(b), the particles have the diameter of about 30 nm, while the rods have the diameter of about 100 nm and length of about 2 μm . For comparison, Fig. 1(c) and (d) shows the selected-area electron diffraction (SAED) patterns of typical individual particle and rod, respectively. According to the standard card of orthorhombic KNbO_3 (JCPDS No. 71-2171), both patterns could be indexed with the orthorhombic Perovskite structure, confirming the same composition for the nano-particles and nano-rods.

Fig. 2 shows the different magnified surface optical photographs of the NKN ceramics sintered at different temperatures. When the sintering temperature reaches 850 °C, there are several black spots appearing in the ceramic surface, which grow gradually with increasing temperature. In order to further confirm the structure of these black spots, the polarizing micrograph of a sample sintered at 950 °C is observed under polarized microscope. As shown in Fig. 3, the same brightness of the black spot testifies the uniform crystal tropism, which confirms that the black spots are abnormal grains. For NKN, the equilibrium crystal shape is cubic, probably with (001) faces.²⁷ If one looks at the (001) plane of such a cube, it would look like a square. However, it can be found in Fig. 2 that the abnormal grains have different shapes, such as square, rectangle and triangular. So, it can be safely concluded that the special grain morphology in our specimen can be attributed to the appearance of different tropism plane, such as (001), (110) and (111) parallel to the ceramic surface.

Fig. 4 presents a typical TEM image of a thinned abnormal grain in the NKN sample sintered at 950 °C. The insert figure shows the corresponding SAED pattern. It can be found that the SAED pattern could be indexed perfectly with the orthorhombic Perovskite structure of NKN, therefore confirming that the abnormal grain is a single crystal form.

The average abnormal grain sizes and number of abnormal grains per cm^2 at different sintering temperatures have been calculated according to Fig. 2(a), and the results are shown in

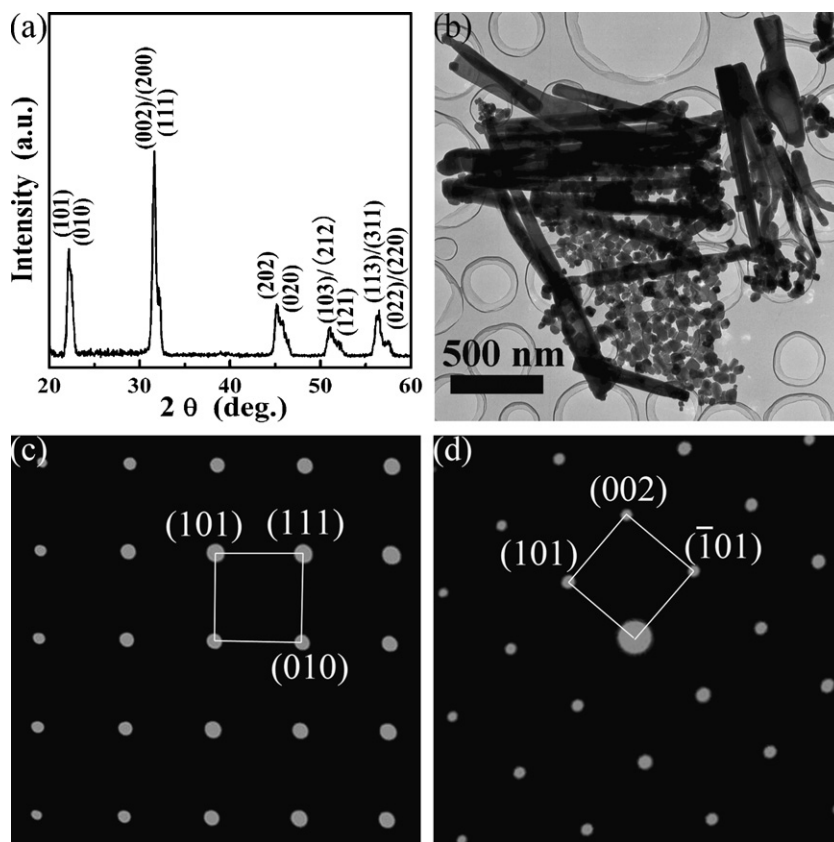


Fig. 1. (a) XRD pattern, (b) TEM image of the NKN powders from sol–gel method, selected-area electron diffraction (SAED) patterns of typical individual particle (c) and rod (d).

Fig. 5(a) and (b), respectively. It can be seen that both curves show the increase trend with the increase of sintering temperature. At 950 °C, the average abnormal grain size is as large as 1.08 mm and the number of abnormal grains gets 50 per cm².

Fig. 6 shows the photograph of some relatively large NKN crystals obtained from samples sintered at 950 °C by mechanical separation. It can be seen in Fig. 6, similar to AGG phenomena in PZT Perovskite ceramics,²⁸ the obtained NKN crystal appears to contain two or three abnormal grains joined together by penetration twins. However, it should be pointed that the big NKN crystal has the large size above 3 mm. Compared with the published data,^{22–24} the relative large size of NKN single crystal can be obtained easily by using AGG method with composite

nano-powders as precursor. From Fig. 6, it can also be found that the growth behavior of the abnormal NKN grains is controlled by means of two-dimensional nucleation, starting at the crystal corners or edges.

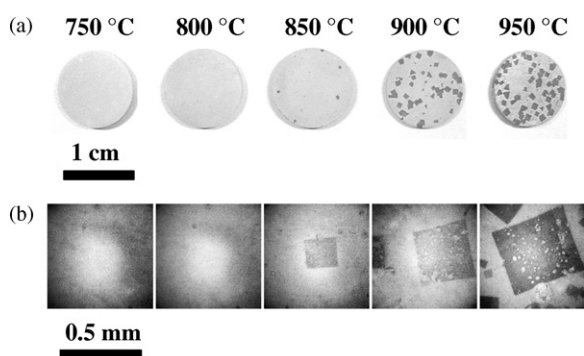


Fig. 2. Surface optical photographs of the NKN ceramics sintered at different temperatures.

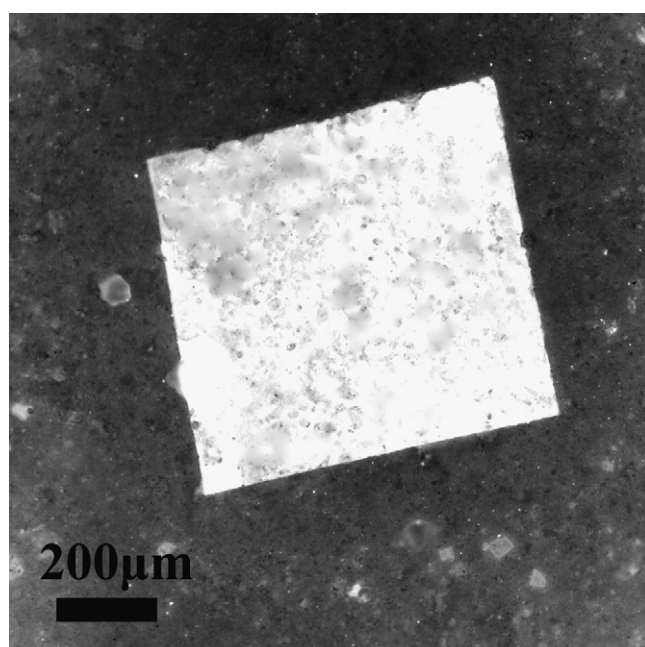


Fig. 3. The polarizing micrograph of a sample sintered at 950 °C.

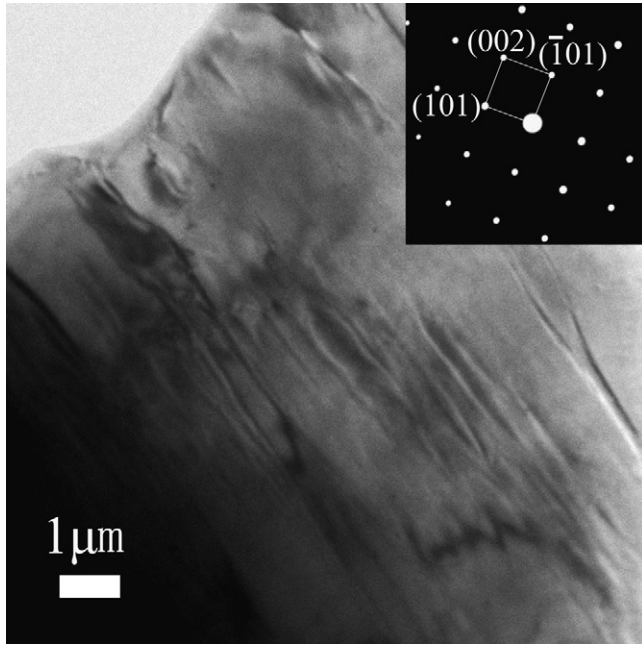


Fig. 4. TEM image and SAED pattern (inset) of an abnormal grain.

For a grain growing by two-dimensional nucleation, the growth rate can be given by²⁹:

$$\dot{R} \cong v_{st} \exp\left(-\frac{\pi\Omega\varepsilon^2}{6\Delta GhkT}\right) \quad (1)$$

where \dot{R} is growth rate, v_{st} is step velocity of the growing nucleus, Ω is molar volume, ε is edge free energy of the nucleus, ΔG is driving force for grain growth, h is step height of the nucleus, k is Boltzman's constant and T is temperature. The driving force of a grain is inversely related to the mean grain radius. Compared to micron-sized powders, nano-sized powders have higher ΔG , which is beneficial to rapid grain growth. For the

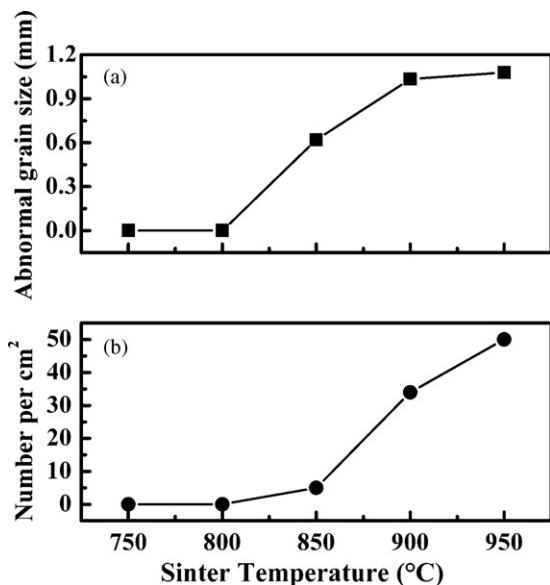


Fig. 5. The dependence of average abnormal grain size (a) and the number of abnormal grains per cm² (b) on the sintering temperature.

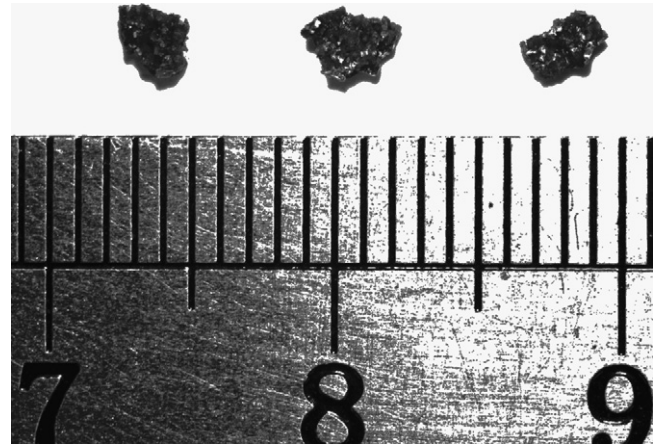


Fig. 6. Optical photograph of some relatively large NKN crystals obtained from samples sintered at 950 °C.

case of a grain growing in the solid-state, the driving force is given by³⁰:

$$\Delta G = \sigma_{gb}\Omega \left(\frac{1}{\bar{r}} - \frac{1}{r}\right) \quad (2)$$

where σ_{gb} is the average grain boundary energy, r is the radius of the growing grain and \bar{r} is the radius of a grain which is neither growing nor shrinking (usually given by the mean grain radius). It can be concluded from the formula above, with the mean grain radius as a constant value, depending on the distribution of grain sizes, the grains will have a range of driving forces for growth. The larger grain will have larger driving force for growth.

Growth of the grain is characterized by two stages: a very slow growth rate at low driving forces, followed by an abnormal rapid growth rate once the driving force exceeds a critical value. The critical driving force is given by²⁹:

$$\Delta G_C = \frac{\Omega\varepsilon^2}{3hkT} \quad (3)$$

Depending on the relative values of ΔG_C and ΔG , the grains will have different types of grain growth behavior, such as slowly growing grains ($\Delta G \leq \Delta G_C$), and abnormal rapidly growing grains ($\Delta G > \Delta G_C$). When sintered at a relatively low temperature (<850 °C), ΔG_C is enhanced to a high value and all the grains have $\Delta G \leq \Delta G_C$. In this case, AGG is depressed and all the grains grow normally. However, because of the different grain sizes, the nano-particles and nano-rods will have different driving forces. The nano-rods have a higher driving force for growth and can grow more rapidly than the nano-particles because the nano-rods are much larger than the nano-particles, and the distribution of the grain sizes in ceramics become extensive. Fig. 7 shows the SEM photograph of the fracture surface for NKN ceramics sintered at 750 °C. The sample is randomly particulate in shape distribution. The small particles are about several hundreds of nanometers while the large grains even develop to the size bigger than 2 μm, which can confirm the extrapolation above. When the samples are sintered at 850 °C, there are more nano-rods with $\Delta G > \Delta G_C$, which are able to grow rapidly to form abnormal grains. With the sintering temper-

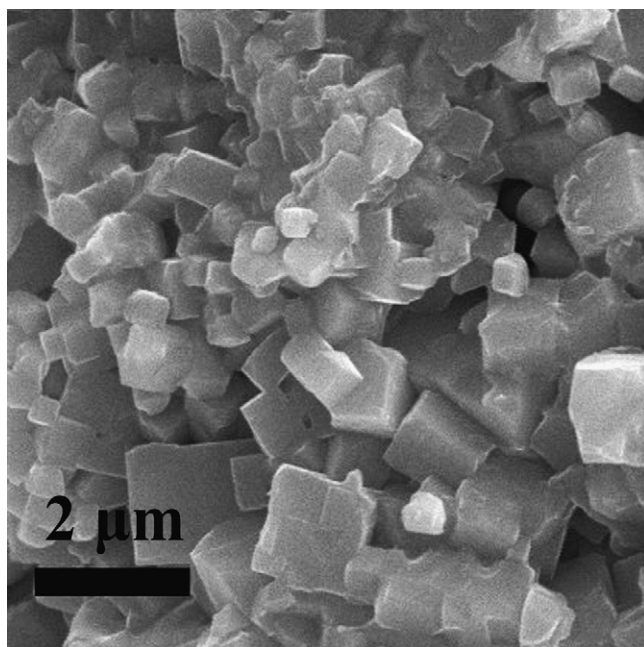


Fig. 7. SEM photograph of the fracture surface for NKN ceramics sintered at 750 °C.

ature increasing to 900 °C, ΔG_C reduces further and the amount of nano-rods with $\Delta G > \Delta G_C$ increases accordingly, cause the average abnormal grain size and the number of abnormal grains per cm^2 increase. Because the amount of nano-rods which are consumed for abnormal grains is limited, with the sintering temperature increasing to 950 °C, compared to the number of abnormal grains per cm^2 , the average abnormal grain size does not increase visibly.

4. Conclusion

Nano-sized $(\text{Na}_{0.5}\text{K}_{0.5})\text{NbO}_3$ powders with composited structure of particles and rods were synthesized by the improved sol–gel method. Using these composite powders as starting materials, millimeter sized NKN single crystals were obtained by AGG method. The biggest NKN single crystals with size of about 3 mm were obtained at 950 °C for 2 h. The analysis of crystal growth mechanism during AGG process revealed that the nano-rods have the larger driving forces compared to that of nano-particles, which grow rapidly especially at high temperature above 850 °C, and finally formed the large NKN single crystals. The method presented in this paper will make preparation of NKN single crystals convenient and greatly reduce the production cost, and thus can be extended to the synthesis of other alkali niobates crystals.

Acknowledgements

This work was partially funded by the Natural Science Foundation of Beijing (Grant No. 2102006), the Project of New Star of Science and Technology of Beijing (Grant no. 2007A014), the Development Project of Science and Technology sponsored by Beijing Education Committee (Grant No. KM200810005012),

the Funding Project for Academic Human Resources Development in Institutions of Higher Learning Under the Jurisdiction of Beijing Municipality, PHR (IHLB) (Grant No. PHR201008012) and the Doctorate Innovation Project of Beijing University of Technology (Grant no. bcx-2009-071).

References

1. Fu HX, Cohen RE. Polarization rotation mechanism for ultrahigh electromechanical response in single-crystal piezoelectrics. *Nature* 2000;**403**:281–3.
2. Guo YP, Luo HS, Ling D, Xu HQ, He TH, Yin ZW. The phase transition sequence and the location of the Morphotropic Phase Boundary region in $(1-x)[\text{Pb}(\text{Mg}_{1/3}\text{Nb}_{2/3})\text{O}_3]-x\text{PbTiO}_3$ single crystal. *J Phys: Condens Matter* 2003;**15**:L77–82.
3. Ge HY, Hou YD, Zhu MK, Wang H, Yan H. Facile synthesis and high d_{33} of single-crystalline KNbO_3 nanocubes. *Chem Commun* 2008;**41**: 5137–9.
4. Chiang YM, Farrey GW, Soukhovjak AN. Lead-free high-strain single-crystal piezoelectrics in the alkaline-bismuth–titanate Perovskite family. *Appl Phys Lett* 1998;**73**:3683–5.
5. Chu BJ, Chen DR, Li GR, Yin QR. Electrical properties of $\text{Na}_{1/2}\text{Bi}_{1/2}\text{TiO}_3$ – BaTiO_3 ceramics. *J Eur Ceram Soc* 2002;**22**:2115–21.
6. Park SE, Chung SJ, Kim IT. Ferroic phase transitions in $(\text{Na}_{1/2}\text{Bi}_{1/2})\text{TiO}_3$ crystals. *J Am Ceram Soc* 1996;**79**:1290–6.
7. Jaeger RE, Egerton L. Hot pressing of potassium–sodium niobates. *J Am Ceram Soc* 1962;**45**:209–13.
8. Saito Y, Takao H, Tani T, Nonoyama T, Takatori K, Homma T, et al. Lead-free piezoceramics. *Nature* 2004;**432**:84–7.
9. Guo YP, Kakimoto K, Ohsato H. Phase transitional behavior and piezoelectric properties of $(\text{Na}_{0.5}\text{K}_{0.5})\text{NbO}_3$ – LiNbO_3 ceramics. *Appl Phys Lett* 2004;**85**:4121–3.
10. Hollenstein E, Davis M, Damjanovic D, Setter N. Piezoelectric properties of Li- and Ta-modified $(\text{K}_{0.5}\text{Na}_{0.5})\text{NbO}_3$ ceramics. *Appl Phys Lett* 2005;**87**:182905-1–3.
11. Chen K, Xu GS, Yang DF, Wang XF, Li JB. Dielectric and piezoelectric properties of lead-free $0.95(\text{K}_{0.5}\text{Na}_{0.5})\text{NbO}_3$ – 0.05LiNbO_3 crystals grown by the Bridgman method. *J Appl Phys* 2007;**101**:044103-1–4.
12. Lin DB, Li ZR, Zhang SZ, Xu Z, Yao X. Dielectric/piezoelectric properties and temperature dependence of domain structure evolution in lead free $(\text{K}_{0.5}\text{Na}_{0.5})\text{NbO}_3$ single crystal. *Solid State Commun* 2009;**149**:1646–9.
13. Kizaki Y, Noguchi Y, Miyayama M. Defect control for superior properties in $\text{K}_{0.5}\text{Na}_{0.5}\text{NbO}_3$ single crystals. *Key Eng Mater* 2007;**350**:85–8.
14. Holden AN. Preparation of metal single crystals. *Trans Am Soc Met* 1950;**42**:319–46.
15. Chen NK, Maddin R, Pond RB. Growth of molybdenum single crystals. *J Met* 1951;**3**:461–4.
16. Yamamoto T, Sakuma T. Fabrication of barium titanate single crystals by solid-state grain growth. *J Am Ceram Soc* 1994;**77**:1107–9.
17. Yoo YS, Kang MK, Han JH, Kim H, Kim DY. Fabrication of BaTiO_3 single crystals by using the exaggerated grain growth method. *J Eur Ceram Soc* 1997;**17**:1725–7.
18. Li T, Scotch AJ, Chan HM, Harmer MP, Park S, Shrout TR, et al. Single crystals of $65\text{Pb}(\text{Mg}_{1/3}\text{Nb}_{2/3})\text{O}_3$ –35 mol% PbTiO_3 from polycrystalline precursors. *J Am Ceram Soc* 1998;**81**:244–8.
19. Fisher JG, Bencan A, Kosec M, Vernay S, Rytz D. Growth of dense single crystals of potassium sodium niobate by a combination of solid-state crystal growth and hot pressing. *J Am Ceram Soc* 2008;**91**:1503–7.
20. Bencan A, Tchernychova E, Godec M, Fisher J, Kosec M. Compositional and structural study of a $(\text{K}_{0.5}\text{Na}_{0.5})\text{NbO}_3$ single crystal prepared by solid state crystal growth. *Microsc Microanal* 2009;**15**:435–40.
21. Lee HY, Kim JS, Kim DY. Fabrication of BaTiO_3 single crystals using secondary abnormal grain growth. *J Eur Ceram Soc* 2000;**20**:1595–7.
22. Zhen YH, Li JF. Abnormal grain growth and new core–shell structure in $(\text{K}, \text{Na})\text{NbO}_3$ -based lead-free piezoelectric ceramics. *J Am Ceram Soc* 2007;**90**:3496–502.

23. Wang YL, Damjanovic D, Klein N, Setter N. High-temperature instability of Li- and Ta-modified (K, Na)NbO₃ piezoceramics. *J Am Ceram Soc* 2008;**91**:1962–70.
24. Fisher JG, Kang S-JL. Microstructural changes in (K_{0.5}Na_{0.5})NbO₃ ceramics sintered in various atmospheres. *J Eur Ceram Soc* 2009;**29**:2581–8.
25. Wang C, Hou YD, Ge HY, Zhu MK, Wang H, Yan H. Sol–gel synthesis and characterization of lead-free LNKN nanocrystalline powder. *J Cryst Growth* 2008;**310**:4635–9.
26. Schatt W, Wieters KP. *Powder metallurgy European powder metallurgy association*. Shrewsbury, UK: Bellstone; 1997.
27. Jenko D, Bencan A, Malic B, Holc J, Kosec M. Electron microscopy studies of potassium sodium niobate ceramics. *Microsc Microanal* 2005;**11**:572–80.
28. Kim KW, Jo W, Jin HR, Hwang NM, Kim DY. Abnormal grain growth of lead zirconium titanate (PZT) ceramics induced by the penetration twin. *J Am Ceram Soc* 2008;**91**:1962–70.
29. Van der Eerden JP. Crystal growth mechanisms. In: Hurlle DTJ, editor. *handbook of crystal growth, fundamentals, Part A, thermodynamics and kinetics*, vol. 1. Amsterdam, Netherlands: Elsevier Science Publishers; 1993. p. 311–475.
30. Yoon DY, Park CW, Koo JB. The step growth hypothesis for abnormal grain growth. In: Yoo HI, Kang S-JL, editors. *Ceramic interfaces 2*. London: Institute of Materials; 2001. p. 3–21.